Gyrotropic Magnetic Effect and the Magnetic Moment on the Fermi Surface

Shudan Zhong,[1] Joel E. Moore,[1,2] and Ivo Souza[3,4]
[1]Department of Physics, University of California, Berkeley, California 94720, USA
[2]Materials Sciences Division, Lawrence Berkeley National Laboratory, Berkeley, California 94720, USA
[3]Centro de Física de Materiales, Universidad del País Vasco, 20018 San Sebastían, Spain
[4]Ikerbasque Foundation, 48013 Bilbao, Spain

(Received 7 October 2015; revised manuscript received 12 December 2015; published 18 February 2016)

The current density $\boldsymbol{j}^{\mathbf{B}}$ induced in a clean metal by a slowly-varying magnetic field $\mathbf{B}$ is formulated as the low-frequency limit of natural optical activity, or natural gyrotropy. Working with a multiband Pauli Hamiltonian, we obtain from the Kubo formula a simple expression for $\alpha_{ij}^{\mathrm{GME}} = j_i^{\mathbf{B}}/B_j$ in terms of the intrinsic magnetic moment (orbital plus spin) of the Bloch electrons on the Fermi surface. An alternate semiclassical derivation provides an intuitive picture of the effect, and takes into account the influence of scattering processes in dirty metals. This "gyrotropic magnetic effect" is fundamentally different from the chiral magnetic effect driven by the chiral anomaly and governed by the Berry curvature on the Fermi surface, and the two effects are compared for a minimal model of a Weyl semimetal. Like the Berry curvature, the intrinsic magnetic moment should be regarded as a basic ingredient in the Fermi-liquid description of transport in broken-symmetry metals.

DOI: 10.1103/PhysRevLett.116.077201

Introduction.—When a solid is placed in a static magnetic field the nature of the electronic ground state can change, leading to striking transport effects. A prime example is the integer quantum Hall effect in a quasi-two-dimensional metal in a strong perpendicular field [1]. Novel magnetotransport effects have also been predicted to occur in 3D topological (Weyl) metals, such as an anomalous longitudinal magnetoresistence [2,3], and the chiral magnetic effect (CME), where an electric pulse $\mathbf{E}\|\mathbf{B}$ induces a transient current $\boldsymbol{j}\|\mathbf{B}$ [4]; both are related to the chiral anomaly that was originally discussed for Weyl fermions in particle physics [5,6]. In all these phenomena the role of the static $\mathbf{B}$ field is to modify the equilibrium state, but an $\mathbf{E}$ field is still required to put the electrons out of equilibrium and drive the current (since $\mathbf{E} = -\dot{\mathbf{A}}$, the vector potential is time dependent even for a static $\mathbf{E}$ field).

Recently, the intriguing proposal was made that a pure $\mathbf{B}$ field could drive a dissipationless current in certain Weyl semimetals where isolated band touchings [the "Weyl points" (WPs)] of opposite chirality are at different energies [7]. The existence of such an effect was later questioned [8], and the initial interpretation as an *equilibrium* current was discounted. (Indeed, that would a violate a "no-go theorem" attributed to Bloch that forbids macroscopic current in a bulk system in equilibrium [9].) Subsequent theoretical work suggests that the proposed effect can still occur in *transport*, as the current response to a $\mathbf{B}$ field oscillating at low frequencies [10–13].

At present the effect is still widely regarded as being related to the chiral anomaly [10] (or, more generally, to the Berry curvature of the Bloch bands [11–14]), and is broadly characterized as a type of CME. We show in this Letter that the experimental implications and microscopic origin of this effect are both very different from the CME (as defined in Ref. [4], consistent with the particle-physics literature [15]). Experimentally, the effect is realized as the low-frequency limit of natural gyrotropy [16] in clean metals (see also Ref. [14]), and we will call it the "gyrotropic magnetic effect" (GME). Both $\mathbf{E}$ and $\mathbf{B}$ optical fields drive the gyrotropic current, but at frequencies well below the threshold for interband absorption ($\hbar\omega \ll \epsilon_{\mathrm{gap}}$) their separate contributions can be identified. In nonpolar metals, the induced gyrotropic current can be inferred from optical rotation measurements. The GME is predicted to occur not only in certain Weyl semimetals, but in any optically active metal; it is necessary that the structure lacks an inversion center, and it is sufficient that the structure is either chiral [17,19,20] or polar [18].

Existing expressions for the natural gyrotropy current in metals involve the Berry curvature of all the occupied states (and velocities of empty bands) [11–14], at odds with the notion that transport currents are carried by states near the Fermi level ϵ_F. Integrals over all occupied states involving the Berry curvature also appear in calculations of a part of the low-frequency optical activity [21–23], and of the anomalous Hall effect (AHE); in the case of the AHE, a Fermi surface (FS) reformulation exists [24]. We find that the GME is not governed by the chiral anomaly or the Berry curvature, but by the intrinsic magnetic moment of the Bloch states on the FS. Our analysis also takes into account the finite relaxation time τ in real materials, which is shown to weaken the effect at the lowest frequencies. The magnitude of the GME is estimated for the predicted chiral Weyl semimetal $SrSi_2$ [25].

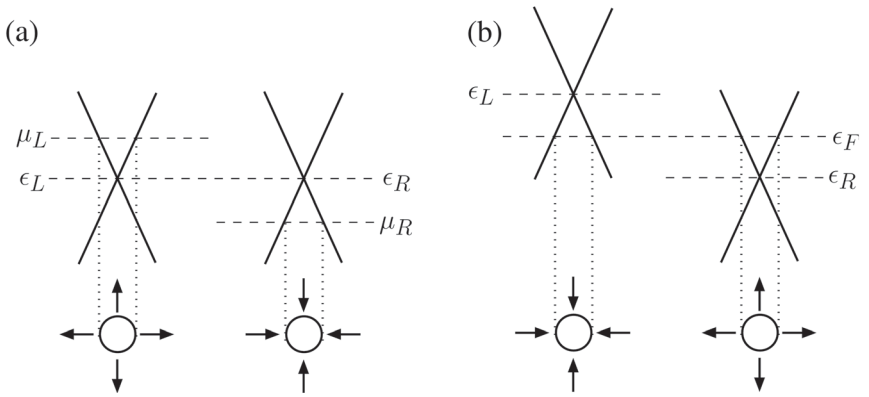

FIG. 1. (a) Chiral magnetic effect in a T-broken Weyl semimetal in a static $\mathbf{B}$ field. The left- and right-handed Weyl nodes are at the same energy $\epsilon_L = \epsilon_R$, but the enclosing Fermi pockets are not in chemical equilibrium ($\mu_L \neq \mu_R$) due to the application of an $\mathbf{E}\|\mathbf{B}$ pulse, and this drives the current [Eq. (3)]. (b) Gyrotropic magnetic effect. P symmetry is now broken along with T, leading to $\epsilon_L \neq \epsilon_R$. The Fermi pockets are in chemical equilibrium, $\mu_L = \mu_R = \epsilon_F$, and an oscillating $\mathbf{B}$ field drives the current [Eq. (17)]. The bottom of each panel shows the Fermi pockets, and the arrows represent the Fermi velocities.

CME versus GME.—Both effects can be discussed by positing a linear relation between $\boldsymbol{j}$ and $\mathbf{B}$:

$$j_i = \alpha_{ij} B_j. \tag{1}$$

Suppose we use linear response to evaluate $\boldsymbol{\alpha}$ for a clean metal, describing the $\mathbf{B}$ field in terms of a vector potential that depends on both $\mathbf{q}$ and ω. The result will depend on the order in which the $\mathbf{q} \to 0$ and $\omega \to 0$ limits are taken [10–12], much as the compressibility and conductivity are different limits of electrical response. The CME tensor $\boldsymbol{\alpha}^{\mathrm{CME}}$ can be obtained from Eq. (1) in the equilibrium or *static* limit of the magnetic field (setting $\omega = 0$ before sending $\mathbf{q} \to 0$), with an additional step needed to describe the $\mathbf{E}$-field pulse. The GME tensor $\boldsymbol{\alpha}^{\mathrm{GME}}$ is extracted directly from Eq. (1) in the transport or *uniform* limit (sending $\mathbf{q} \to 0$ before $\omega \to 0$) that describes conductivities in experiment. (Here, "$\omega \to 0$" means $\hbar\omega \ll \epsilon_{\mathrm{gap}}$, but note that $\omega\tau \gg 1$ because the clean limit $\tau \to \infty$ is assumed; effects caused by finite relaxation times in dirty samples will be discussed later.) Only $\boldsymbol{\alpha}^{\mathrm{GME}}$ is a material property, since the details of the $\mathbf{E}$-field pulse producing nonequilibrium are missing from $\boldsymbol{\alpha}^{\mathrm{CME}}$. Below we derive microscopic expressions for both.

Chiral magnetic effect.—The tensor $\boldsymbol{\alpha}$ calculated in the static limit is isotropic, $\alpha_{ij} = \alpha^{\mathrm{stat}}\delta_{ij}$, with

$$\alpha^{\mathrm{stat}} = -\frac{e^2}{\hbar}\sum_n \int [d\mathbf{k}] f^0_{\mathbf{k}n}(\mathbf{v}_{\mathbf{k}n}\cdot\Omega_{\mathbf{k}n}) = 0, \tag{2}$$

where $[d\mathbf{k}] = d^3k/(2\pi)^3$, the integral is over the Brillouin zone, $f^0_{\mathbf{k}n} = f(\epsilon_{\mathbf{k}n})$ is the equilibrium occupation factor, $\mathbf{v}_{\mathbf{k}n} = \partial_{\hbar\mathbf{k}}\epsilon_{\mathbf{k}n}$ is the band velocity, $\Omega_{\mathbf{k}n} = -\mathrm{Im}\langle\partial_{\mathbf{k}}u_{\mathbf{k}n}| \times |\partial_{\mathbf{k}}u_{\mathbf{k}n}\rangle$ is the Berry curvature, and $-e$ is the electron charge. Equation (2) was derived in Ref. [26] using the semiclassical formalism [27], and we obtain the same result from linear response [28]. The fact that α^{stat} vanishes (see below) is in accord with Bloch's theorem [9].

To turn the above "quasiresponse" into α^{CME}, let us recast Eq. (2) as a FS integral. Integrating by parts produces two terms. The one containing $\partial_{\mathbf{k}}\cdot\Omega_{\mathbf{k}n}$ picks up monopole contributions from the occupied WPs, and vanishes because each WP appears twice with opposite signs [44]. In the remaining term we write $\partial_{\mathbf{k}}f^0 = -\hat{\mathbf{v}}_F\delta^3(\mathbf{k}-\mathbf{k}_F)$, with $\hat{\mathbf{v}}_F$ the FS normal at $\mathbf{k}_F$, and introduce the Chern number $C_{na} = (1/2\pi)\int_{S_{na}} dS(\hat{\mathbf{v}}_F\cdot\Omega_{\mathbf{k}n})$ of the ath Fermi sheet S_{na} in band n [24,44]. After assigning different chemical potentials to different sheets to account for the effect of the $\mathbf{E}$-field pulse, Eq. (2) becomes $\alpha^{\mathrm{CME}} = -(e^2/h^2)\sum_{n,a}\mu_{na}C_{na}$, leading to the current density $\boldsymbol{j} = \alpha^{\mathrm{CME}}\mathbf{B}$ [4,9]. In equilibrium $\mu_{na} = \epsilon_F$, and using $\sum_{n,a}C_{na} = 0$ we find $\boldsymbol{j} = 0$, as per Eq. (2).

For a Weyl semimetal with two Fermi pockets with $C = +1$ and $C = -1$ placed at slightly different chemical potentials μ_L and μ_R [45] [Fig. 1(a)], a current develops:

$$\boldsymbol{j} = (e^2/h^2)\mathbf{B}(\mu_R - \mu_L). \tag{3}$$

Gyrotropic magnetic effect.—Symmetry considerations already suggest a link between the GME and natural gyrotropy. Both $\boldsymbol{j}$ and $\mathbf{B}$ are odd under time reversal T, and $\boldsymbol{j}$ is odd under spatial inversion P, while $\mathbf{B}$ is P even, and so according to Eq. (1) the GME is T even and P odd, the same as natural gyrotropy [16].

To make the connection precise, consider the current density induced by a monochromatic electromagnetic field $\mathbf{A}(t,\mathbf{r}) = \mathbf{A}(\omega,\mathbf{q})e^{i(\mathbf{q}\cdot\mathbf{r}-\omega t)}$ at first order in $\mathbf{q}$:

$$j_i(\omega,\mathbf{q}) = \Pi_{ijl}(\omega)A_j(\omega,\mathbf{q})q_l. \tag{4}$$

The T-even part Π^A_{ijl} of the response tensor is antisymmetric (A) under $i \leftrightarrow j$. It has nine independent components, and can be repackaged as a rank-2 tensor using [46,47]

$$\Pi^A_{ijl} = i\varepsilon_{ilp}\alpha^{\mathrm{GME}}_{jp} - i\varepsilon_{jlp}\alpha^{\mathrm{GME}}_{ip}, \tag{5a}$$

$$\alpha^{\mathrm{GME}}_{ij} = \frac{1}{4i}\varepsilon_{jlp}(\Pi^A_{lpi} - 2\Pi^A_{ilp}). \tag{5b}$$

At nonabsorbing frequencies $\boldsymbol{\alpha}^{\mathrm{GME}}(\omega)$ is real and $\boldsymbol{\Pi}^A(\omega)$ is purely imaginary, but otherwise both are complex.

From now on we assume $\hbar\omega \ll \epsilon_{\rm gap}$, so that only intraband absorption can occur. In this regime $\boldsymbol{\alpha}^{\rm GME}$ satisfies

$$j_i^{\mathbf{B}} = -i\omega P_i^{\mathbf{B}} = \alpha_{ij}^{\rm GME} B_j, \tag{6a}$$

$$M_i^{\mathbf{E}} = -(i/\omega)\alpha_{ji}^{\rm GME} E_j, \tag{6b}$$

where $\mathbf{E} = i\omega\mathbf{A}$ and $\mathbf{B} = i\mathbf{q}\times\mathbf{A}$, and $\mathbf{P}^{\mathbf{B}}$ and $\mathbf{M}^{\mathbf{E}}$ are oscillating moments induced by $\mathbf{B}$ and $\mathbf{E}$, respectively. The natural gyrotropy current is $\boldsymbol{j}^{\mathbf{B}} + i\mathbf{q}\times\mathbf{M}^{\mathbf{E}}$. In the long-wavelength limit Eq. (6a) describes a transport current induced by a time-varying $\mathbf{B}$ in an optically active metal (the *direct* GME), and Eq. (6b) describes a macroscopic magnetization induced by $\mathbf{E}$; this *inverse* GME has been previously discussed for polar [48] and chiral [49] metals.

To derive Eq. (6), consider a finite sample of size L. Using Eq. (20) of Ref. [47] for $\sigma_{ijl}^A = (1/i\omega)\Pi_{ijl}^A$, we find [50]

$$\alpha_{ij}^{\rm GME} = (\omega/2i)(\chi_{ij}^{\rm em} - \chi_{ji}^{\rm me}) + (\text{E.Q. terms}). \tag{7}$$

"E. Q." denotes electric quadrupole terms that keep $\boldsymbol{\alpha}^{\rm GME}$ origin independent at higher frequencies [47,51], but do not contribute to $\boldsymbol{j}^{\mathbf{B}}$ or $\mathbf{M}^{\mathbf{E}}$ when $\hbar\omega \ll \epsilon_{\rm gap}$, as they are higher order in ω than the first term. The low-frequency gyrotropic response is controlled by the magnetoelectric susceptibilities $\chi_{ij}^{\rm em} = \partial P_i/\partial B_j$ and $\chi_{ij}^{\rm me} = \partial M_i/\partial E_j$. The dynamic polarization $P_i^{\mathbf{B}}$ can be decomposed into T-even and T-odd parts $(1/2)(\chi_{ij}^{\rm em} - \chi_{ji}^{\rm me})B_j$ and $(1/2)(\chi_{ij}^{\rm em} + \chi_{ji}^{\rm me})B_j$ [52], and Eq. (6a) corresponds to the former. Similarly, Eq. (6b) gives the T-even part of the magnetization induced by $\mathbf{E}$. (The T-odd part of the magnetoelectric susceptibilities describes the linear magnetoelectric effect in insulators such as Cr_2O_3.)

In brief, the GME is the low-frequency limit of natural gyrotropy in P-broken metals, in much the same way that the AHE is the transport limit of Faraday rotation in T-broken metals. While the intrinsic AHE is governed by the geometric Berry curvature [24,27] and becomes quantized by topology in Chern insulators, the GME is controlled by a nongeometric quantity, the intrinsic magnetic moment of the Bloch states on the FS [54].

To establish this result let us return to periodic crystals and derive a bulk formula for $\boldsymbol{\alpha}^{\rm GME}$ at $\hbar\omega \ll \epsilon_{\rm gap}$. From the Kubo linear response in the uniform limit, we obtain [28]

$$\Pi_{ijl}^A = \frac{e^2\omega\tau}{1-i\omega\tau}\sum_n \int [d\mathbf{k}]\frac{\partial f}{\partial\epsilon_{\mathbf{k}n}}\left[-\frac{g_s}{2m_e}\varepsilon_{ipl}v_{\mathbf{k}n,j}S_{\mathbf{k}n,p} + \frac{v_{\mathbf{k}n,i}}{\hbar}\mathrm{Im}\langle\partial_j u_{\mathbf{k}n}|H_{\mathbf{k}} - \epsilon_{\mathbf{k}n}|\partial_l u_{\mathbf{k}n}\rangle - (i\leftrightarrow j)\right]. \tag{8}$$

[The calculation was carried out for a clean metal where formally $\tau = 1/\eta$ and $\eta \to 0^+$ [56]. Alternately one could retain a finite τ to give a phenomenological relaxation time in dirty metals, and indeed the semiclassical relaxation-time calculation to be presented shortly gives the same Drude-like dependence on $\omega\tau$ as Eq. (8)]. $\mathbf{S}_{\mathbf{k}n}$ is the expectation value of the spin $\mathbf{S} = (\hbar/2)\boldsymbol{\sigma}$ of a Bloch state, $g_s \simeq 2$ is the spin g factor of the electron, and m_e is the electron mass. Inserting Eq. (8) into Eq. (5b) gives

$$\alpha_{ij}^{\rm GME} = \frac{i\omega\tau e}{1-i\omega\tau}\sum_n \int [d\mathbf{k}](\partial f/\partial\epsilon_{\mathbf{k}n})v_{\mathbf{k}n,i}m_{\mathbf{k}n,j}, \tag{9}$$

where $\mathbf{m}_{\mathbf{k}n} = -(eg_s/2m_e)\mathbf{S}_{\mathbf{k}n} + \mathbf{m}_{\mathbf{k}n}^{\rm orb}$ is the magnetic moment of a Bloch electron, whose orbital part is [27]

$$\mathbf{m}_{\mathbf{k}n}^{\rm orb} = \frac{e}{2\hbar}\mathrm{Im}\langle\partial_{\mathbf{k}}u_{\mathbf{k}n}|\times(H_{\mathbf{k}} - \epsilon_{\mathbf{k}n})|\partial_{\mathbf{k}}u_{\mathbf{k}n}\rangle. \tag{10}$$

At zero temperature, we can replace $\partial f/\partial\epsilon_{\mathbf{k}n}$ in Eq. (9) with $-\delta^3(\mathbf{k}-\mathbf{k}_F)/\hbar|\mathbf{v}_{\mathbf{k}n}|$ to obtain the FS formula

$$\alpha_{ij}^{\rm GME} = \frac{i\omega\tau}{i\omega\tau - 1}\frac{e}{(2\pi)^2 h}\sum_{n,a}\int_{S_{na}} dS\hat{v}_{F,i}m_{\mathbf{k}n,j}. \tag{11}$$

A nonzero $\mathbf{m}_{\mathbf{k}n}$ requires broken PT symmetry, but the GME can only occur if P is broken: with P symmetry present, $\mathbf{m}_{-\mathbf{k},n} = \mathbf{m}_{\mathbf{k}n}$ and $\hat{\mathbf{v}}_F(-\mathbf{k}_F) = -\hat{\mathbf{v}}_F(\mathbf{k}_F)$, leading to $\boldsymbol{\alpha}^{\rm GME} = 0$. Without spin-orbit coupling, only the orbital moment contributes.

Equations (6) and (11) are our main results. The GME is fully controlled by the bulk FS and vanishes trivially for insulators, contrary to the AHE where the FS formulation misses possible quantized contributions [24].

According to Eq. (11), the reactive response $\mathrm{Re}\boldsymbol{\alpha}^{\rm GME}$ is suppressed by scattering when $\omega \ll 1/\tau$. It increases with ω, and levels off for $\omega \gg 1/\tau$ (satisfying this condition without violating $\hbar\omega \ll \epsilon_{\rm gap}$ requires sufficiently clean samples). The opposite is true for the dissipative response $\mathrm{Im}\boldsymbol{\alpha}^{\rm GME}$, which drops to zero at $\omega \gg 1/\tau$ and becomes strongest at $\omega \ll 1/\tau$. In this lowest-frequency limit $\boldsymbol{j}^{\mathbf{B}} \to 0$, and Eqs. (6b) and (9) for the induced magnetization reduce to the expression in Ref. [49]. Thus, in the dc limit only a dissipative inverse GME occurs in dirty metals.

Semiclassical picture.—Our discussion of the GME assumed from the outset $\hbar\omega \ll \epsilon_{\rm gap}$. Since this is the regime where the semiclassical description of transport in metals holds [57], it is instructive to rederive Eqs. (6) and (9) by solving the Boltzmann equation. This provides an intuitive picture of the GME and its modification by scattering processes. The key ingredient beyond previous semiclassical approaches [21–23] is the correction to the band energy and the band velocity (as opposed to the anomalous velocity) in the presence of a magnetic field [12,27]: $\tilde{\mathbf{v}}_{\mathbf{k}n} = \partial_{\hbar\mathbf{k}}\tilde{\epsilon}_{\mathbf{k}n}$, where $\tilde{\epsilon}_{\mathbf{k}n} = \epsilon_{\mathbf{k}n} - \mathbf{m}_{\mathbf{k}n}\cdot\mathbf{B}$.

In a static $\mathbf{B}$ field, the conduction electrons reach a new equilibrium state with $f_{\mathbf{k}n}^0(\mathbf{B}) = f(\tilde{\epsilon}_{\mathbf{k}n})$ as the distribution function [12], and the current vanishes according to Eq. (2). Under oscillating fields $\mathbf{E}, \mathbf{B} \propto e^{i(\mathbf{q}\cdot\mathbf{r}-\omega t)}$ the electrons are in an excited state with a distribution function $g_{\mathbf{k}n}(t,\mathbf{r})$

which we find by solving the Boltzmann equation in the relaxation-time approximation,

$$\partial_t g_{\mathbf{k}n} + \dot{\mathbf{r}}\frac{\partial g_{\mathbf{k}n}}{\partial \mathbf{r}} + \dot{\mathbf{k}}\frac{\partial g_{\mathbf{k}n}}{\partial \mathbf{k}} = -[g_{\mathbf{k}n} - f^0_{\mathbf{k}n}(\mathbf{B})]/\tau, \quad (12)$$

where τ is the relaxation time to return to the instantaneous equilibrium state described by $f^0_{\mathbf{k}n}(\mathbf{B}(t,\mathbf{r}))$ (for a slow spatial variation of $\mathbf{B}$). Using the semiclassical equations [27], the distribution function to linear order in $\mathbf{E}$ and $\mathbf{B}$ is $g_{\mathbf{k}n}(t,\mathbf{r}) = f^0_{\mathbf{k}n}(\mathbf{B}(t,\mathbf{r})) + f^1_{\mathbf{k}n}(t,\mathbf{r})$, with

$$f^1_{\mathbf{k}n} = \frac{\partial f/\partial \epsilon_{\mathbf{k}n}}{1 - \frac{\mathfrak{q}}{\omega}\cdot \mathbf{v}_{\mathbf{k}n} + \frac{i}{\omega\tau}}[\mathbf{m}_{\mathbf{k}n}\cdot\mathbf{B} + (ie/\omega)\mathbf{E}\cdot\mathbf{v}_{\mathbf{k}n}], \quad (13)$$

which at $\omega\tau \gg 1$ reduces to the result in Ref. [12].

As the current associated with $f^0_{\mathbf{k}n}(\mathbf{B})$ vanishes, the current induced by an oscillating $\mathbf{B}$ field is obtained by multiplying the first term in Eq. (13) with the unperturbed band velocity. The result in the long-wavelength limit is

$$\boldsymbol{j}^{\mathbf{B}} = \frac{i\omega\tau e}{1 - i\omega\tau}\sum_n \int [d\mathbf{k}](\partial f/\partial\epsilon_{\mathbf{k}n})\mathbf{v}_{\mathbf{k}n}(\mathbf{m}_{\mathbf{k}n}\cdot\mathbf{B}), \quad (14)$$

in agreement with Eqs. (6a) and (9). Conversely, inserting the second term of Eq. (13) in the bulk expression for $\mathbf{M} = \mathbf{M}^{\rm spin} + \mathbf{M}^{\rm orb}$ [27] leads to Eqs. (6b) and (9) for the magnetization induced by an oscillating $\mathbf{E}$ field.

GME in two-band models.—Consider a situation where only two bands are close to ϵ_F, and couplings to more distant bands can be neglected when evaluating the orbital moment on the FS (for simplicity, we focus here on the orbital contribution). The Hamiltonian written in the basis of the identity matrix and the three Pauli matrices is $H_{\mathbf{k}} = \bar{\epsilon}_{\mathbf{k}}\mathbb{1} + \mathbf{d}_{\mathbf{k}}\cdot\boldsymbol{\sigma}$, with eigenvalues $\epsilon_{\mathbf{k}t} = \bar{\epsilon}_{\mathbf{k}} + td_{\mathbf{k}}$, where $t = \pm 1$ and $d_{\mathbf{k}} = |\mathbf{d}_{\mathbf{k}}|$. Equation (10) becomes

$$m^{\rm orb}_{\mathbf{k}t,i} = -\frac{e}{\hbar}\varepsilon_{ijl}\frac{1}{2d^2_{\mathbf{k}}}\mathbf{d}_{\mathbf{k}}\cdot(\partial_j\mathbf{d}_{\mathbf{k}}\times\partial_l\mathbf{d}_{\mathbf{k}}). \quad (15)$$

For orientation we study a minimal model for a Weyl semimetal where the FS consists of two pockets surrounding isotropic WPs of opposite chirality. We allow the WPs to be at different energies (this requires breaking both P and T), but ϵ_F is assumed close to both [Fig. 1(b)]. Near each WP the Hamiltonian is $H_{\mathbf{k}\nu} = \epsilon_\nu\mathbb{1} + \chi_\nu\hbar v_F\mathbf{k}\cdot\boldsymbol{\sigma}$, where ν labels the WP, ϵ_ν and $\chi_\nu = \pm 1$ are its energy and chirality (positive means right-handed), $\mathbf{k}$ is measured from the WP, and v_F is the Fermi velocity. From Eq. (15), $\mathbf{m}^{\rm orb}_{\mathbf{k}\nu} = -\chi_\nu(ev_F/2k)\hat{\mathbf{k}}$ for $t = \pm 1$, and only the trace piece $\bar{\alpha}^{\rm GME}\delta_{ij}$ survives in Eq. (11); in the clean limit each pocket contributes

$$\bar{\alpha}^{\rm GME}_\nu = \mp\frac{1}{3}\frac{e^2}{h^2}\chi_\nu\hbar v_F k_F = \frac{1}{3}\frac{e^2}{h^2}\chi_\nu(\epsilon_\nu - \epsilon_F), \quad (16)$$

where the minus (plus) sign in the middle expression corresponds to $\epsilon_\nu < \epsilon_F$ ($\epsilon_\nu > \epsilon_F$). Summing over ν and using $\sum_\nu\chi_\nu = 0$ [58] gives $\bar{\alpha}^{\rm GME} = (e^2/3h^2)\sum_\nu\chi_\nu\epsilon_\nu$. For a minimal model $\nu = L, R$, and the GME current is

$$\boldsymbol{j}^{\mathbf{B}} = (e^2/3h^2)(\epsilon_R - \epsilon_L)\mathbf{B}. \quad (17)$$

Equation (17) looks deceptively similar to Eq. (3) for the CME current. The prefactor is different, but the key difference is in the meaning of the various quantities, and in their respective roles. To stress this point, in both equations we have placed the "force" that drives the current at the end, after the equilibrium parameter that enables the effect. The GME current is driven by the oscillating $\mathbf{B}$ field, while ϵ_L and ϵ_R are band structure parameters, with $\epsilon_R - \epsilon_L$ reflecting the degree of structural symmetry breaking that allows the effect to occur. Equation (3) is "universal" because of the topological nature of the FS integral involved, while Eq. (17) is for spherical pockets surrounding isotropic Weyl nodes. For generic two-band models the traceless part of $\boldsymbol{\alpha}^{\rm GME}$ is generally nonzero [59], and the non-FS expression of Refs. [11,12] for the orbital contribution to the trace can be recovered from Eq. (9) [28].

We emphasize that breaking T is not required for the GME. If T is present (and P broken), the minimum number of WPs is four, not two [60]. In the class of T-symmetric Weyl materials so far discovered, T relates WPs of the same chirality and energy. Mirror symmetries connect WPs of opposite chirality so that $\boldsymbol{j}^{\mathbf{B}}\cdot\mathbf{B} = 0$, as expected since these symmetries tend to exclude optical rotation [19,20]. Fortuitously, the predicted Weyl material $SrSi_2$ has misaligned WPs of opposite chirality due to broken mirror symmetry [25]. Its rotatory power ρ can be estimated from the energy splitting between WPs. Neglecting anisotropy effects and spin contributions that were not included in Eq. (17), each WP pair contributes [28]

$$\rho = (2\alpha/3hc)(\epsilon_L - \epsilon_R), \quad (18)$$

with α the fine-structure constant and c the speed of light. The calculated splitting $|\epsilon_L - \epsilon_R| \sim 0.1$ eV [25] gives $|\rho| \sim 0.4$ rad/mm per node pair, about the same as $|\rho| = 0.328$ rad/mm for quartz at $\lambda = 0.63\,\mu$m [20]. This should be measurable in a frequency range from the infrared (above which the semiclassical assumptions break down) down to $1/\tau$, which depends on crystal quality. When $\epsilon_L = \epsilon_R$ the rotatory power vanishes in equilibrium, but a nonequilibrium gyrotropic effect can still occur due to the chiral anomaly [22,28]. In polar metals, the tensor $\boldsymbol{\alpha}^{\rm GME}$ acquires an antisymmetric part (equivalent to a polar vector $\boldsymbol{\delta}$) that does not contribute to optical rotation, but which leads to a *transverse* GME of the form $\mathbf{M}^{\mathbf{E}} \propto \mathbf{E}\times\boldsymbol{\delta}$ [28].

In summary, we have elucidated the physical origin of currents induced by low-frequency magnetic fields in metals in terms of the magnetic moment on the FS, and discussed the experimental implications. Unlike the CME [61] or the photoinduced AHE [62], no detailed model of

nonequilibrium is required to quantify the GME, and efficient *ab initio* methods already exist to compute the needed orbital moments [63].

We thank Q. Niu, J. Orenstein, D. Pesin, and D. Vanderbilt for useful comments, and also thank D. Vanderbilt for calling our attention to Ref. [49] and suggesting a possible connection with the present work. We acknowledge support from Grant No. NSF DMR-1507141 (S. Z.), from the DOE LBL Quantum Materials Program and Simons Foundation (J. E. M.), and from Grants No. MAT2012-33720 from the Spanish Ministerio de Economía y Competitividad and No. CIG-303602 from the European Commission (I. S.).

Note added.—Along with the present paper, the role of orbital moments in the natural gyrotropy of metals was also recognized in Ref. [64].

[1] D. J. Thouless, M. Kohmoto, M. P. Nightingale, and M. den Nijs, Phys. Rev. Lett. **49**, 405 (1982).
[2] H. B. Nielsen and M. Ninomiya, Phys. Lett. **130B**, 389 (1983).
[3] D. T. Son and B. Z. Spivak, Phys. Rev. B **88**, 104412 (2013).
[4] D. T. Son and N. Yamamoto, Phys. Rev. Lett. **109**, 181602 (2012).
[5] S. Adler, Phys. Rev. **177**, 2426 (1969).
[6] J. S. Bell and R. Jackiw, Nuovo Cimento A **60**, 47 (1969).
[7] A. A. Zyuzin, S. Wu, and A. A. Burkov, Phys. Rev. B **85**, 165110 (2012).
[8] M. M. Vazifeh and M. Franz, Phys. Rev. Lett. **111**, 027201 (2013).
[9] N. Yamamoto, Phys. Rev. D **92**, 085011 (2015).
[10] Y. Chen, S. Wu, and A. A. Burkov, Phys. Rev. B **88**, 125105 (2013).
[11] P. Goswami and S. Tewari, arXiv:1311.1506.
[12] M.-C. Chang and M.-F.Yang, Phys. Rev. B **91**, 115203 (2015).
[13] M.-C. Chang and M.-F. Yang, Phys. Rev. B **92**, 205201 (2015).
[14] P. Goswami, G. Sharma, and S. Tewari, Phys. Rev. B **92**, 161110(R) (2015).
[15] D. E. Kharzeev, Prog. Part. Nucl. Phys. **75**, 133 (2014).
[16] The term *natural gyrotropy* refers to the time-reversal-even part of the optical response of a medium at linear order in the wave vector of light [17,18]. The reactive part gives rise to natural optical rotation, and the dissipative part to natural circular dichroism. Furthermore, polar crystals display natural gyrotropy effects unrelated to optical rotation [18]. Gyrotropic effects that are time-reversal-odd and zeroth order in the wave vector of light (e.g., Faraday rotation and magnetic circular dichroism [17]) are not considered in this work.
[17] L. D. Landau and E. M. Lifshitz, *Electrodynamics of Continuous Media*, 2nd ed. (Pergamon Press, Oxford, 1984).
[18] V. M. Agranovich and V. L. Ginzburg, *Crystal Optics with Spatial Dispersion, and Excitons*, 2nd ed. (Springer, Berlin, 1984).
[19] H. D. Flack, Helv. Chim. Acta **86**, 905 (2003).
[20] R. E. Newnham, *Properties of Materials* (Oxford University Press, Oxford, 2005).
[21] J. Orenstein and J. E. Moore, Phys. Rev. B **87**, 165110 (2013).
[22] P. Hosur and X.-L. Qi, Phys. Rev. B **91**, 081106 (2015).
[23] S. Zhong, J. Orenstein, and J. E. Moore, Phys. Rev. Lett. **115**, 117403 (2015).
[24] F. D. M. Haldane, Phys. Rev. Lett. **93**, 206602 (2004).
[25] S.-M. Huang, S.-Y. Xu, I. Belopolski, C.-C. Lee, G. Chang, B. Wang, N. Alidoust, M. Neupane, H. Zheng, D. Sanchez, A. Bansil, G. Bian, H. Lin, and M. Z. Hasan, arXiv:1503.05868.
[26] J.-H. Zhou, J. Hua, Q. Niu, and J.-R. Shi, Chin. Phys. Lett. **30**, 027101 (2013).
[27] D. Xiao, M.-C. Chang, and Q. Niu, Rev. Mod. Phys. **82**, 1959 (2010).
[28] See Supplemental Material at http://link.aps.org/supplemental/10.1103/PhysRevLett.116.077201, which includes Refs. [29–43], for (i) the derivation of Eqs. (2) and (8) from linear response, (ii) the derivation from Eq. (9) of the non-FS formula for $\bar{\alpha}^{\mathrm{GME}}$ given in Refs. [11,12], (iii) the derivation of Eq. (18) from Eq. (17) combined with phenomenological relations, (iv) an analysis of the gyrotropic response in polar metals, and of the gyrotropic reponse induced in Weyl semimetals by the chiral anomaly, (v) the derivation of a reciprocity relation for the natural gyrotropy of a metal with a smooth interface, and (vi) the identification of a traceless Berry-curvature piece in the full GME response tensor of Eq. (9).
[29] E. I. Blount, Solid State Phys. **13**, 305 (1962).
[30] Y. Yafet, Solid State Phys. **14**, 1 (1963).
[31] F. Wooten, *Optical Properties of Solids* (Academic Press, New York, 1972).
[32] M. Dressel and G. Grüner, *Electrodynamics of Solids* (Cambridge University Press, Cambridge, UK, 2002).
[33] W. A. Harrison, *Solid State Theory* (Dover, New York, 1980).
[34] W. Yao, D. Xiao, and Q. Niu, Phys. Rev. B **77**, 235406 (2008).
[35] K. Natori, J. Phys. Soc. Jpn. **39**, 1013 (1975).
[36] P. Hosur, A. Kapitulnik, S. A. Kivelson, J. Orenstein, and S. Raghu, Phys. Rev. B **87**, 115116 (2013).
[37] L. Barron, *Molecular Light Scattering and Optical Activity* (Cambridge University Press, Cambridge, UK, 2004).
[38] B. Halperin, in The Physics and Chemistry of Oxide Superconductors, *Springer-Verlag Proceedings of Physics* Vol. 60, edited by Y. Iye and H. Yasuoka (Springer-Verlag, Berlin, 1992), p. 439.
[39] A. D. Fried, Phys. Rev. B **90**, 121112 (2014).
[40] V. M. Agranovich and V. I. Yudson, Opt. Commun. **9**, 58 (1973).
[41] V. V. Bokut and A. N. Serkyukov, Zh. Prikl. Spectrosk. **20**, 677 (1974) [J. Appl. Spectrosc. **20**, 513 (1974)].
[42] A. P. Vinogradov, Phys. Usp. **45**, 331 (2002).
[43] N. P. Armitage, Phys. Rev. B **90**, 035135 (2014).
[44] D. Gosálbez-Martínez, I. Souza, and D. Vanderbilt, Phys. Rev. B **92**, 085138 (2015).
[45] With our sign convention for the Berry curvature, a right-handed WP acts as a source in the lower band and as a sink in the upper band [27]. An enclosing pocket, either electron-like or holelike, has Chern number $C = -1$.

[46] R. M. Hornreich and S. Shtrikman, Phys. Rev. **171**, 1065 (1968).
[47] A. Malashevich and I. Souza, Phys. Rev. B **82**, 245118 (2010).
[48] V. M. Edelstein, Phys. Rev. B **83**, 113109 (2011), and references therein.
[49] T. Yoda, T. Yokoyama, and S. Murakami, Sci. Rep. **5**, 12024 (2015).
[50] To recover the bulk result from Eq. (7), the $L \to \infty$ limit should be taken faster than the $\omega \to 0$ limit, consistent with the order of limits discussed earlier for transport.
[51] A. D. Buckingham and M. D. Dunn, J. Chem. Soc. A, 1988 (1971).
[52] This decomposition is obtained by invoking the Onsager relation $\chi^{\mathrm{em}}_{ij}(\omega)|_{-\mathbf{B}_{\mathrm{ext}}} = -\chi^{\mathrm{me}}_{ji}(\omega)|_{\mathbf{B}_{\mathrm{ext}}}$ [53].
[53] D. B. Melrose and R. C. McPhedran, *Electromagnetic Processes in Dispersive Media* (Cambridge University Press, Cambridge, United Kingdom, 1991).
[54] Here, the term *geometric* refers to the intrinsic geometry of the Bloch-state fiber bundle. The orbital moment of Bloch electrons can be considered geometric in a different sense: it is the imaginary part of a complex tensor whose real part gives the inverse effective mass tensor, i.e., the curvature of band dispersions [55].
[55] Y. Gao, S. A. Yang, and Q. Niu, Phys. Rev. B **91**, 214405 (2015).
[56] P. B. Allen, in Conceptual Foundations of Materials Properties: A Standard Model for Calculation of Ground- and Excited-State Properties, *Contemporary Concepts of Condensed Matter Science* Vol. 1, edited by S. G. Louie and M. L. Cohen (Elsevier, New York, 2006), p. 165.
[57] N. W. Ashcroft and N. D. Mermin, *Solid State Physics* (Brooks-Cole, Belmont, MA, 1976).
[58] H. Nielsen and M. Ninomiya, Nucl. Phys. **B185**, 20 (1981).
[59] For any number of bands, the traceless part of $\boldsymbol{\alpha}^{\mathrm{GME}}$ includes [28] the Berry-curvature piece found previously [23], and the full tensor satisfies [28] the microscopic constraint from time-reversal symmetry previously shown for that traceless piece.
[60] S. M. Young, S. Zaheer, J. C. Y. Teo, C. L. Kane, E. J. Mele, and A. M. Rappe, Phys. Rev. Lett. **108**, 140405 (2012).
[61] S. A. Parameswaran, T. Grover, D. A. Abanin, D. A. Pesin, and A. Vishwanath, Phys. Rev. X **4**, 031035 (2014).
[62] K. F. Mak, K. L. McGill, J. Park, and P. L. McEuen, Science **344**, 1489 (2014).
[63] M. G. Lopez, D. Vanderbilt, T. Thonhauser, and I. Souza, Phys. Rev. B **85**, 014435 (2012).
[64] J. Ma and D. A. Pesin, Phys. Rev. B **92**, 235205 (2015).